2009 American Control Conference
Hyatt Regency Riverfront, St. Louis, MO, USA
June 10-12, 2009

Second Order Sliding Mode for Traction Control in Ride-by-Wire Sport Motorcycles

Claudio Vecchio, Mara Tanelli, Matteo Corno, Antonella Ferrara, Sergio M. Savaresi

Abstract— **The paper addresses the analysis and design of a safety-oriented traction control system for ride-by-wire sport motorcycles via Second Order Sliding Mode (SOSM) techniques. The controller design is based on a nonlinear dynamical model of the rear wheel slip, and the modeling phase is validated against experimental data measured on an instrumented vehicle. To comply with practical applicability constraints, the position of the electronic throttle body is used as control variable and the effect of the actuator dynamics thoroughly analyzed. After a discussion on the interplay between the controller parameters and the tracking performance, the final design effectiveness is assessed via MSC BikeSim®, a full-fledged commercial multibody motorcycle model.**

I. Introduction and Motivation

Nowadays, four-wheeled vehicles are equipped with many different active control systems which enhance driver's and passengers' comfort and safety. In the field of two-wheeled vehicles, instead, the development of electronic control systems is still in its infancy. However, the importance of active control for traction and braking has been recently recognised also in the motorcycle context, [1]. The motivation for this is twofold: on one hand, in the racing context, these systems are designed to enhance vehicle performance; on the other hand, in the production context, the same control systems are intended to enhance the safety of non-professional bikers, whose number is steadily increasing mainly due to traffic congestion and high oil price.

To the best of the Authors' knowledge, little or no previous work has been done on the problem of rear wheel slip dynamics analysis and Traction Control (TC) for two-wheeled vehicles, whereas the same problem has been addressed on four-wheeled vehicles in e.g., [2], [3]. TC increases safety and performance by controlling the slip of the rear (driving) wheel. As is well known, the wheel slip is related to the force exerted by the tire via the friction curves, [4], [5]. By keeping the slip of the tire on the peak of the longitudinal curve, one achieves the best performance and at the same time improves safety. If the peak is surpassed there is only a marginal loss of longitudinal force but a dramatic loss of lateral force that could cause a fall during cornering.

It is worth noting that, as far as control systems design is concerned, dealing with motorcycle dynamics is far more subtle than it is for four-wheeled vehicles. In fact, it is common practice to design most active control systems for cars based on simplified dynamical models (*e.g.*, the quarter-car model and the half-car model for braking control systems and the single-track model for active stability control, [4]), while complete vehicle models are employed mostly for testing and validation phases. In two-wheeled vehicles, instead, the presence of a single axle, together with the peculiar suspensions, steer and fork geometry, makes it difficult to devise appropriate simplified models. The effort of analyzing well-defined driving conditions seems to be the key for a comprehensive control design for motorcycles. Such an approach is well confirmed in the scientific literature of this field (see *e.g.*, [5], [6].

This paper addresses the analysis and design of a safety-oriented traction control system for ride-by-wire sport motorcycles via Second Order Sliding Mode (SOSM) techniques. The sliding mode control methodology is chosen because of its robustness properties, which make it particularly suitable to deal with the system uncertainties and the wide range of operating conditions typical of the automotive context [7]. Furthermore, SOSM controllers feature higher accuracy with respect to first order sliding mode control, and generate continuous control actions, since the discontinuity is confined to the derivative of the control signal, thereby reducing actuator stress and wear [7], [8]. Apart from the robustness features against possible disturbances and parameter variations affecting the vehicle model, the sliding mode control methodology has also the advantage of producing low complexity control laws compared to other robust control approaches which appears particularly suitable to be implemented in the Electronic Control Unit (ECU) of a controlled vehicle [7], [8].

II. Dynamical Model

For the preliminary design of traction control algorithms in motorcycles, we are interested in modeling the rear wheel slip dynamics. To this aim, focusing on straight-line traction maneuvers, the following dynamical model can be employed

$$J_r\dot{\omega}_r = -r_r F_{x_r} + T \tag{1}$$

$$J_f\dot{\omega}_f = -r_f F_{x_f} \tag{2}$$

$$m\dot{v} = F_{x_r} + F_{x_f}, \tag{3}$$

where ω_f [rad/s] and ω_r [rad/s] are the angular speeds of the front and rear wheel, respectively, v [m/s] is the longitudinal speed of the vehicle body, T [Nm] is the driving torque,

C. Vecchio and A. Ferrara are with the Department of Computer Engineering and Systems Science, University of Pavia, Via Ferrata 1, 27100 Pavia, Italy. E-mail:{antonella.ferrara,claudio.vecchio}@unipv.it. M. Tanelli, M. Corno and S.M. Savaresi are with the Dipartimento di Elettronica e Informazione, Politecnico di Milano, Piazza Leonardo da Vinci 32, 20133 Milano, Italy. E-mail:{tanelli,corno,savaresi}@elet.polimi.it. M. Tanelli is also with the Dipartimento di Ingegneria dell'Informazione e Metodi Matematici, Università degli studi di Bergamo, Via Marconi 5, 24044, Dalmine (BG), Italy.The work of M. Tanelli, M. Corno and S.M. Savaresi has been partially supported by MIUR project "New methods for Identification and Adaptive Control for Industrial Systems".

F_{x_f} and F_{x_r} [N] are the front and rear longitudinal tire-road contact forces, $J_f = J_r = J$ [kgm^2], m [kg] and $r_f = r_r = r$ [m] are the wheel inertias, the vehicle mass, and the wheel radii, respectively. Note that, for simplicity, the front and rear wheel inertias and the wheel radii are assumed to be equal and indicated with J and r, respectively. The system is nonlinear due to the dependence of F_{x_i}, $i = \{f, r\}$, on the state variables v and ω_i, $i = \{f, r\}$. The expression of F_{x_i} as a function of these variables is involved and influenced by a large number of features of the road, tire, and suspension; however, it can be well-approximated as follows (see [4])

$$F_{x_i} = F_{z_i}\, \mu(\lambda_i, \beta_{i_t}; \vartheta), \quad i = \{f, r\}, \tag{4}$$

where F_{z_i} is the vertical force at the tire-road contact point and $\mu(\cdot, \cdot; \vartheta)$ is a function of

- the longitudinal slip $\lambda_i \in [0, 1]$, which, during traction, is defined as

$$\lambda_i = \frac{\omega_i r - v}{\omega_i r}; \tag{5}$$

- the wheel side-slip angle β_{i_t}.

Vector ϑ in $\mu(\cdot, \cdot; \vartheta)$ represents the set of parameters that identify the tire-road friction condition. Since for traction maneuvers performed along a straight line one can set the wheel side-slip angle equal to zero ($\beta_{i_t} = 0$), we shall omit the dependence of F_{x_i} on β_{i_t} and denote the μ function as $\mu(\cdot; \vartheta)$.

Remark 2.1: It is worth mentioning that the results in this work remain valid if we remove the assumption that $\beta_{i_t} = 0$. In fact, changes in β_{i_t} cause a shift in the peak position of the $\mu(\cdot; \vartheta)$ curve and act as a scaling factor (in this resembling the effect of changes in the vertical load). Accordingly, as the controller is designed assuming no knowledge both of the current road conditions and of the value of the vertical load, it can handle non-zero values of β_{i_t}. ■

Many empirical analytical expressions for function $\mu(\cdot; \vartheta)$ have been proposed in the literature. A widely-used expression (see [4]) is

$$\mu(\lambda; \vartheta) = \vartheta_1(1 - e^{-\lambda\vartheta_2}) - \lambda\vartheta_3, \tag{6}$$

where ϑ_i, $i = 1, 2, 3$, are the three components of vector ϑ. By changing the values of these three parameters, many different tire-road friction conditions can be modeled. the shape of $\mu(\lambda; \vartheta)$ in four different conditions is displayed. From now on, for ease of notation, the dependency of μ on ϑ will be omitted, and the function in equation (6) will be referred to as $\mu(\lambda)$.

Note, in passing, that from (6) one has that the longitudinal force produced by a wheel is bounded, i.e.,

$$|F_{xi}| \leq \Psi, \qquad i \in \{f, r\}. \tag{7}$$

The tire model (6) is a steady–state model of the interaction between the tire and the road. As for the transient tire behavior we assume that, being it due to tire relaxation dynamics, [4], the traction forces F_{xi} have a bounded first time derivative, i.e.,

$$|\dot{F}_{xi}| \leq \Gamma, \qquad i \in \{f, r\}. \tag{8}$$

By employing system (1)–(3), we are interested in highlighting the rear wheel slip dynamics. To this aim, in order to use the wheel slip definition in (5), a measure or a reliable estimate of the vehicle speed is needed. As is discussed in [9] for the case of braking control, vehicle speed estimation for two-wheeled vehicle is an open problem.

For traction control purposes, however, the problem of vehicle speed estimation is eased by the fact that the only driven wheel is the rear one, so that, in principle, the front wheel linear speed should provide a reasonable estimate of the vehicle speed. Again, the suspension and pitch dynamics, which in two-wheeled vehicles are much more coupled with longitudinal dynamics than they are in cars, should warn that the use of the front wheel speed might provide non precise speed estimates in very strong acceleration phases. However, as in practice no alternative (or more accurate) vehicle speed estimate has been made available yet, we introduce the definition of the *relative* rear wheel slip, namely

$$\lambda_{r,r} = \frac{\omega_r r - \omega_f r}{\omega_r r}, \tag{9}$$

which is nothing but equation (5) with $\omega_f r$ replacing v. This quantity is what can be actually measured on commercial motorbikes. Along this line, we call *absolute* rear wheel slip $\lambda_{r,a}$ the quantity computed as in (5) using the true vehicle speed v.

In what follows it is assumed that the longitudinal dynamics of the vehicle (expressed by the state variable v) are significantly slower than the rotational dynamics of the wheels (expressed by the state variables λ_i or ω_i) due to the differences in inertia. Henceforth, v is considered as a slowly time-varying parameter when analyzing the evolution in time of λ_i (see *e.g.*, [10]). Under this assumption, equation (3) (center of mass dynamics) is neglected, and the model reduces to that of the wheels dynamics only. Further, in system (1)–(3) the state variables are v and ω_i. As λ_i, v and ω_i are linked by the algebraic equation (5), it is possible to replace ω_i with λ_i as state variable. Specifically, let us analyze the *absolute* rear wheel slip $\lambda_{r,a}$. Considering equations (1) and (3) (the front wheel dynamics only affects the vehicle speed equation in the rear slip to torque dynamic relation), and considering the absolute slip definition in (5) together with the longitudinal force description in (4), the absolute rear wheel slip dynamics can be written as

$$\dot{\lambda}_{r,a} = \frac{v}{\omega_r^2 r}\dot{\omega}_r - \frac{1}{\omega_r r}\dot{v} = -\frac{(1-\lambda_{r,a})^2 r}{Jv}\Big\{ [rF_{z_r}\mu(\lambda_{r,a}) - T] \tag{10}$$

$$+ \frac{J}{r\, m\, (1-\lambda_{r,a})}\left(F_{z_r}\mu(\lambda_{r,a}) + F_{z_f}\mu(\lambda_f)\right)\Big\}.$$

In what follows, the SOSM controller will be designed according to the absolute wheel slip dynamics. However, its intrinsic robustness properties will allow to employ the same controller also when the relative wheel slip is used as controlled variable, as will be shown in Section V.

Even though the SOSM controller is designed based on the

nonlinear wheel slip dynamics, in order to be able of validating the analytical model against the frequency response estimates obtained based on experimental data collected on an instrumented vehicle (see Section IV), we are also interested in linearizing the slip dynamics to obtain a transfer function description.

To this aim, we work on the absolute slip dynamics in (10) and start by computing the system equilibria. Thus, we let $\dot{\lambda}_{r,a} = 0$ and look for the equilibrium points characterized by a constant longitudinal slip value $\lambda_{r,a} = \bar{\lambda}_{r,a}$ (note that the equilibrium characterized by $\mu(\lambda) = 0$ and $T = 0$ is meaningless for traction control purposes as it corresponds to the coasting-down condition with no torque applied). From equation (10) it is easy to find that the equilibrium values for the driving torque T are given by

$$\bar{T} = rF_{z_r}\mu(\bar{\lambda}_{r,a}) + \frac{J}{rm(1-\lambda_{r,a})}\left(F_{z_r}\mu(\lambda_{r,a}) + F_{z_f}\mu(\lambda_f)\right). \tag{11}$$

According to the assumption of regarding v as a slowly varying parameter, we can linearize the model around an equilibrium point defined by $\delta T = T - \bar{T}$ and $\delta\lambda_{r,a} = \lambda_{r,a} - \bar{\lambda}_{r,a}$. Defining the slope of the $\mu(\lambda)$ curve around an equilibrium point as

$$\mu_1(\bar{\lambda}) := \left.\frac{\partial\mu(\lambda)}{\partial\lambda}\right|_{\lambda=\bar{\lambda}},$$

the linearized absolute wheel slip dynamics have the form

$$\begin{aligned}\delta\dot{\lambda}_{r,a} = \Bigg\{ & \frac{F_{z_r}}{\bar{v}}\left[\frac{2(1-\bar{\lambda}_{r,a})}{J}r^2 + \frac{1}{m}\right]\mu(\bar{\lambda}_{r,a}) \\ & + \left[\frac{(1-\bar{\lambda}_{r,a})^2 F_{z_r}}{\bar{v}}\left(\frac{r^2}{J} + \frac{1}{m}\right)\right]\mu_1(\bar{\lambda}_{r,a}) \\ & + \frac{\bar{\lambda}_{r,a}}{m\bar{v}}F_{z_f}\mu(\bar{\lambda}_f) - \frac{2(1-\bar{\lambda}_{r,a})r}{J\bar{v}}\bar{T}\Bigg\}\delta\lambda_{r,a} \\ & + \frac{(1-\bar{\lambda}_{r,a})^2 r^2}{\bar{v}}\delta T.\end{aligned} \tag{12}$$

From the linearized dynamics (12) it is immediate to derive the expression of the first-order transfer function $G_{\lambda_{r,a}}(s)$, which will be employed in Section IV for model validation against experimental data.

III. The traction controller design

As previously mentioned, due to the high nonlinearity of the considered system and to the presence of time–varying parameters and uncertainties, which arise from the wide range of operating conditions typical of the automotive context, the control system is designed relying on SOSM control. Due to its robustness feature SOSM methodology results particular suitable to deal with the considered nonlinear uncertain system.

The main advantage of SOSM control [7], with respect to the first order case, is that it can generate continuous control actions, while keeping the same robustness properties with respect to matched uncertainties [11], and a comparable design simplicity.

In this setting the SOSM controller will be designed based on the nonlinear absolute rear slip dynamics only, disregarding at this stage the actuator dynamics (see Section IV). This allows to work on a plant with relative degree one, and to carry out the control design based on standard SOSM theory. The effect of the actuator dynamics will be taken into account in the simulations, and its impact on the closed-loop system analyzed in Section V. The traction controller is designed to steer the rear wheel slip $\lambda_{r,a}$ to the desired value λ_r^*. The error between the current slip and the desired slip is chosen as the sliding variable, i.e.,

$$s_{r,a} = \lambda_{r,a} - \lambda_r^*, \tag{13}$$

and the control objective is to design a continuous control law $\mathcal{T}$ capable of steering this error to zero in finite time. Then, the chosen sliding manifold is given by

$$s_{r,a} = 0 \tag{14}$$

The first and second derivatives of the sliding variable $s_{r,a}$ are

$$\begin{cases} \dot{s}_{r,a} &= \dot{\lambda}_{r,a} - \dot{\lambda}^*_{r,a} \\ \ddot{s}_{r,a} &= \varphi_{r,a} + h_{r,a}\dot{\mathcal{T}}_r \end{cases} \tag{15}$$

where $\dot{\lambda}_{r,a}$ is given by (10), and h_r and φ_r are defined as

$$h_{r,a} := \frac{v}{J\omega_r^2 r} = \frac{(1-\lambda_{r,a})^2 r}{Jv} \tag{16}$$

$$\begin{aligned}\varphi_{r,a} := & -\frac{\ddot{v}}{r\omega_r} + 2\frac{\dot{v}\dot{\omega}_r}{r\omega_r^2} - 2\frac{v\dot{\omega}_r^2}{r\omega_r^3} - \ddot{\lambda}^*_{r,a} - \frac{v\dot{F}_{x_r}}{J\omega_r^2} \\ = & \frac{r(1-\lambda_{r,a})^2}{Jv}\Bigg\{\frac{2(-rF_{x_r}+T)}{v}[m(F_{x_f}+F_{x_r}) \\ & - r(1-\lambda_{r,a})(-rF_{x_r}+T)] - r\dot{F}_{x_r} \\ & - \frac{J(\dot{F}_{x_r}+\dot{F}_{x_f})}{rm(1-\lambda_{r,a})}\Bigg\} - \ddot{\lambda}^*_{r,a}.\end{aligned} \tag{17}$$

Combining (3) with (7) yields

$$|\dot{v}| \leq \frac{2\Psi}{m} = f_1. \tag{18}$$

Further, taking into account the first time derivative of (3), (8), and (18), one has that

$$|\ddot{v}| \leq \frac{2\Gamma}{m} = f_2. \tag{19}$$

Finally, from equations (1) and (7), one gets

$$|\dot{\omega}_r| \leq \frac{-r\Psi + T}{J} = f_3(T). \tag{20}$$

Relying on (18), (19), and (20), and assuming – as it is the case in traction maneuvers – $v > 0$, $\omega_r > 0$ and $\lambda_{r,a} \in [0, 1)$ one has that $\varphi_{r,a}$ is bounded. From a physical viewpoint, this means that, when a constant driving torque T is applied, the second time derivative of the rear wheel slip is bounded.

Note that in order to design a SOSM controller it is not necessary that a precise evaluation of $\varphi_{r,a}$ is available. In the sequel of the paper it will be only assumed that a suitable bound of $\varphi_{r,a}$, i.e.,

$$|\varphi_{r,a}| \leq \Phi_r(v, \omega_r, T) \tag{21}$$

is known. Similar considerations can be made for $h_{r,a}$ which can be regarded as an unknown bounded function with the following known bounds

$$0 < \Gamma_{r1}(v, \omega_r) \leq h_{r,a} \leq \Gamma_{r2}(v, \omega_r). \tag{22}$$

In order to design a second order sliding mode control law, introduce the auxiliary variables $y_1 = s_{r,a}$ and $y_2 = \dot{s}_{r,a}$. Then, system (15) can be rewritten as

$$\dot{y}_1 = y_2, \quad \dot{y}_2 = \varphi_{r,a} + h_{r,a}\dot{\mathcal{T}}, \tag{23}$$

where $\dot{\mathcal{T}}$ is regarded as the auxiliary control input [7]. As a consequence, the control problem can be reformulated as follows: given system (23), where $\varphi_{r,a}$ and $h_{r,a}$ satisfy (21) and (22), respectively, and y_2 is unavailable for measurement, design the auxiliary control signal $\dot{\mathcal{T}}$ so as to steer y_1, y_2 to zero in finite time.

The SOSM controller proposed herein is of sub–optimal type [7]. This implies that, under the assumption of being capable of detecting the extremal values s_{r_M} of the signal $y_1 = s_{r,a}$, the following result can be proved (see also [8]).

Theorem 1: Given system (23), where $\varphi_{r,a}$ and $h_{r,a}$ satisfy (21) and (22), respectively, and y_2 is not measurable, the auxiliary control law

$$\begin{aligned} \dot{\mathcal{T}} &= -\eta V_r \, sign\left(s_{r,a} - \frac{1}{2}s_{rM}\right) \\ \eta &= \begin{cases} \eta^* & \text{if} \quad [s_{r,a} - s_{rM}/2]s_{rM} > 0 \\ 1 & \text{if} \quad [s_{r,a} - s_{rM}/2]s_{rM} \leq 0 \end{cases} \end{aligned} \tag{24}$$

where V_r is the control gain, η is the so–called modulation factor, and s_{rM} is a piece–wise constant function representing the value of the last singular point of $s_r(t)$ (i.e., the most recent value s_{rM} such that $\dot{s}_{r,a}(t_M) = 0$), causes the convergence of the system trajectory on the sliding manifold $s_{r,a} = \dot{s}_{r,a} = 0$ in finite time provided that the control parameters η^* and V_r are chosen so as to satisfy the following constraints

$$\eta^* \in (0, 1] \cap \left(0, \frac{3\Gamma_{r1}}{\Gamma_{r2}}\right) \tag{25}$$

$$V_r > \max\left\{\frac{\Phi_r}{\eta_r^*\Gamma_{r1}}, \frac{4\Phi_r}{3\Gamma_{r1} - \eta^*\Gamma_{r2}}\right\} \tag{26}$$

IV. The complete motorcycle traction dynamics

To better evaluate the suitability for TC design of the dynamical model presented in Section II, we compare it to data collected on a hypersport motorbike which has been used to perform experiments tailored to the identification of actual rear wheel slip dynamics. The considered motorbike is propelled by a 1000cc 4-stroke engine; it weights about 160 kg (without rider) and can deliver more than 200 HP. For confidentiality reasons other details of the motorbike are kept undisclosed. The vehicle is equipped with: an Electronic Throttle Body (ETB) which allows to electronically control the position of the throttle valve independently from the rider's request; an Electronic Control Unit (ECU) that allows to control the throttle. The clock frequency of the ECU is 1 kHz; two wheel encoders to measure the wheels angular velocity and a 1-dimensional optical velocity sensor. This sensor measures the true longitudinal velocity and it will be used to compute the instantaneous absolute rear wheel slip. In order to identify the slip dynamics, frequency sweep response has been employed. The test was carried out on a 3.5 km straight dry asphalt patch; the rider is asked to bring the motorcycle to a given constant engine speed in a given gear. After steady state conditions are reached, the rider presses a button which commences the trial. The throttle control is taken over by the ECU and the excitation signal (a frequency sweep) is applied around the neighborhood of the initial condition. In the following reference is made to the absolute rear wheel slip $\lambda_{r,a}$, which is defined as in (5).

From the experiments, the throttle set point position θ^o and the absolute rear wheel slip $\lambda_{r,a}$ are recorded to estimate the frequency response $\hat{G}_{\lambda_{r,a}}(j\omega)$. Such a non parametric estimate of the frequency response is obtained by windowed spectral analysis of the input/output cross-spectral densities, and is shown with the dashed line in Figure 1. For confidentiality reasons, the frequencies in Figure 1 are shown normalized with respect to the closed loop frequency of the servo-loop throttle control (ω_c).

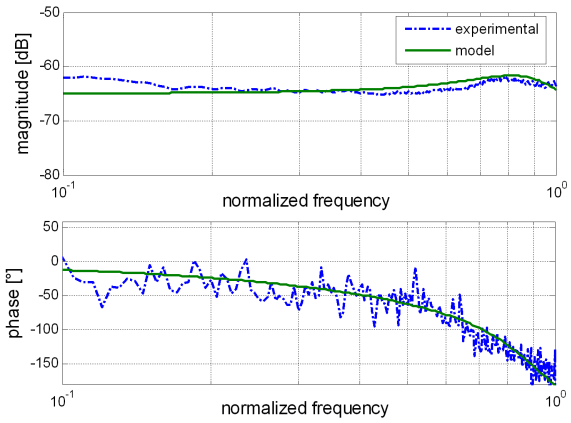

Fig. 1. Experimental frequency response (dashed line) and analytical transfer function (solid line) from throttle set-point to rear wheel slip.

From Figure 1 it can be observed that the measured slip dynamics has a resonance around 0.7-0.8 ω_c. The fact that this resonance is visible also on the engine speed (not shown for space constraints) suggests that it is due to the transmission elasticity.

As such, to complement the analytical wheel slip model (12) so that it accounts for the additional dynamic elements which emerge in the measured data, we need to consider the actuator dynamics and the transmission elasticity.The considered actuator is an Electronic Throttle Body (ETB), which is comprised of butterfly valves actuated by an electrical motor through a reduction system. For traction control purposes, we are interested in modeling the dynamics of the controlled ETB, which, as discussed in [12], can be described as

$$G_{ETB}(s) = \nu(\omega_e)\frac{1}{\tau s + 1}e^{-ds}, \tag{27}$$

that is a first-order low-pass filter with time-varying gain $\nu(\omega_e)$ – where ω_e is the engine speed – and a pure delay d. For modeling the transmission elasticity, a mass-spring-damper description has been chosen, which can be therefore represented by means of the following

$$G_{transm}(s) = \frac{\omega_n^2}{s^2 + 2\xi\omega_n s + \omega_n^2}, \tag{28}$$

where the natural frequency $\omega_n = \sqrt{k/m}$ and $\xi = c/2\sqrt{k\,m}$ and m, c and k are the mass, damping coefficient and spring stiffness of the transmission, respectively.
Thus, the overall analytical model is

$$G_{traction}(s) = G_{th}(s)\, G_{\lambda_{r,a}}(s)\, G_{transm}(s),$$

and it is given by the cascade of the controlled ETB dynamics (27), the transmission (28) and the analytical transfer function $G_{\lambda_{r,a}}(s)$ derived from the linearized model (12). The overall transfer function is shown with the solid line in Figure 1. As can be appreciated, the fitting between measured data and the analytical model can be regarded as quite satisfactory.

V. Simulation Results

This section is devoted to assess the performance of the SOSM controller via a simulation study. We start with a relatively simple Simulink-based in-plane motorcycle model [9], which takes into account tire elasticity and tire relaxation dynamics and models the ETB dynamics. As such, we analyze the controller performance in presence of the actuator dynamics, which have been neglected in the controller design. Then, we investigate the controller robustness when the relative wheel slip is used as controlled variable. Further, we provide a sensitivity analysis of the controller performance with respect to the SOSM controller gain V_r, which allows to highlight interesting trade-offs between tracking performance and settling time. Then, to validate the proposed SOSM controller in a setting as close as possible to real on-bike experiments, we present some simulation results obtained on a full-fledged commercial motorcycle simulator (the Mechanical Simulation Corp. MSC BikeSim® simulation environment, based on the AutoSim symbolic multibody software, which also models transmission and engine dynamics and provides a very accurate description of the road-tire interaction forces, [13].

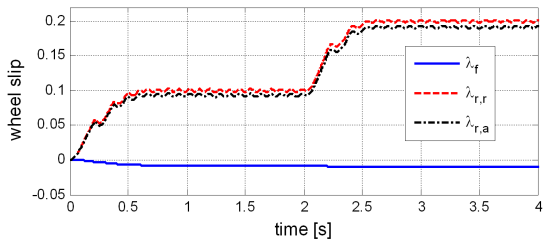

Fig. 2. Plot of relative (dashed line), absolute (dash-dotted line) rear wheel slip and front (solid line) wheel slip in traction maneuver where the slip set-point is changed from $\lambda_r^* = 0.1$ to $\lambda_r^* = 0.2$ at $t = 2$s with relative rear slip $\lambda_{r,r}$ as controlled variable.

Figure 2 shows the time histories of the closed-loop absolute rear wheel slip, vehicle and wheel speeds and driving torque in a traction maneuver where the slip set-point is changed from $\lambda_r^* = 0.1$ to $\lambda_r^* = 0.2$ at $t = 2$s with relative rear slip $\lambda_{r,r}$ as controlled variable. Inspecting Figure 2, note that the wheel slip exhibits small oscillations: analyzing the period of such oscillations one finds that it corresponds to the actuator bandwidth. Such oscillations are due to the fact that the presence of the unmodelled ETB dynamic increases the relative degree of the system (note that the pure delay in (27) has been modeled via a second order Padé approximation, hence with no additional increase in the relative degree). As a consequence, the transient process converge to a periodic motion [14]. However, the amplitude of such oscillations is very small and can be well tolerated in the specific application. Instead, the use of a higher order SM controller – which would be needed in principle to formally deal with a plant with relative degree higher than one – is not advisable in automotive control, as higher order derivatives of the controlled variable need to be computed and this cannot be done reliably due to measurements noise.

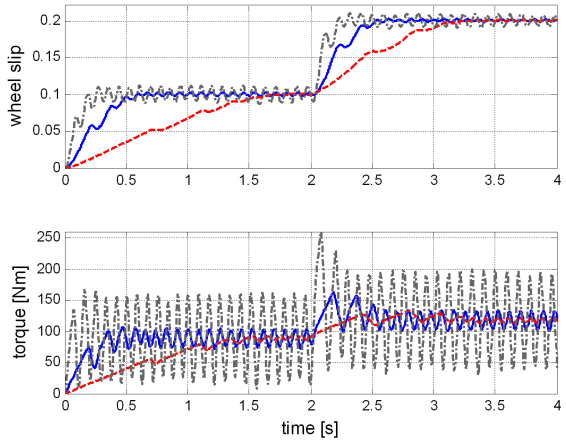

Fig. 3. Plot of (top): relative rear wheel slip; (bottom): driving torque in a traction maneuver where the slip set-point is changed from $\lambda_r^* = 0.1$ to $\lambda_r^* = 0.2$ at $t = 2$s with relative rear slip $\lambda_{r,r}$ as controlled variable and with controller gains V_r (solid line), $5\,V_r$ (dash-dotted line) and $0.2\,V_r$ (dashed line).

It is interesting to investigate the closed-loop system sensitivity with respect to the SOSM controller gain. To this end, refer to Figure 3, where the relative rear wheel slip and the driving torque is shown with nominal controller gain values V_r, increased gain $5\,V_r$ and reduced gain $0.2\,V_r$. What emerges from these results is a clear trade-off between the actuator-induced oscillations amplitude and settling time. Increasing the controller gain by a factor of 5 (see the dash-dotted line in Figure 3), we can nearly halve the settling time, but the price to pay are larger oscillations. The converse holds for the case of decreased gain values (dashed-line in the same figure). This feature is quite interesting for the considered application. As a matter of fact, acceleration maneuvers on slippery roads are much more difficult to handle at low speeds. In fact, the rear wheel slip dynamics are inversely proportional to the vehicle speed, as can be seen in equation

(10). As such, the slip dynamics get faster – hence more difficult to control for human drivers – as speed decreases. Thus, at low speeds one would willingly lose tracking performance in exchange for increased (and guaranteed) safety. The design of an adaptive SOSM controller, where the gains are tuned according to the vehicle speed, is topic of ongoing work.

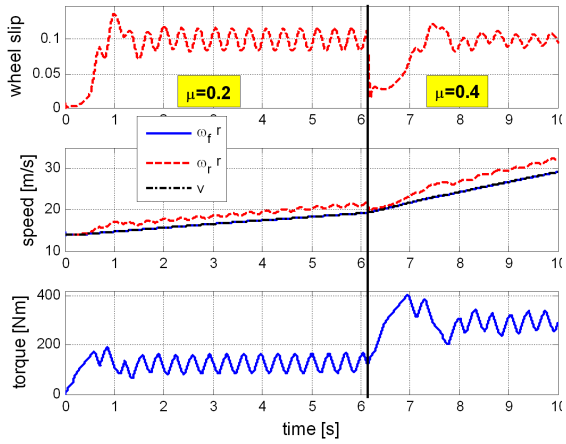

Fig. 4. Plot of (top): relative rear wheel slip; (middle): front wheel (solid line) rear wheel (dashed line) and vehicle (dash-dotted line) speed; (bottom): driving torque in a traction maneuver on the full multibody simulator where a μ-jump from $\mu = 0.2$ to $\mu = 0.4$ with relative rear slip $\lambda_{r,r}$ as controlled variable.

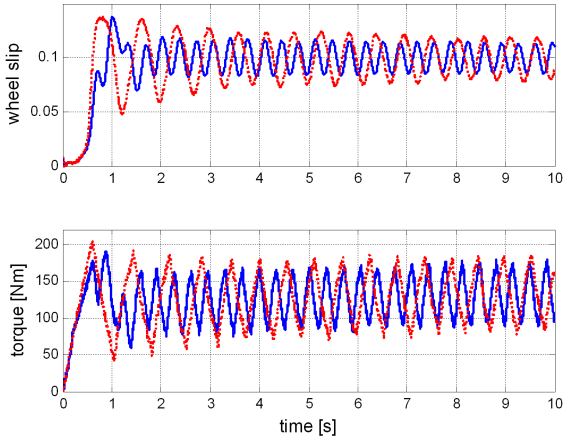

Fig. 5. Plot of (top): relative rear wheel slip; (bottom): driving torque in a traction maneuver on the full multibody simulator with relative rear slip $\lambda_{r,r}$ as controlled variable and matched disturbances, on the throttle position (solid line) and both matched and unmatched disturbances (dotted line).

We now move to assess the controller performance on the full multibody simulator MSC BikeSim®.

To consider challenging yet realistic situations, note that in traction control applications it is crucial that the control algorithm can correctly manage sudden changes in the road conditions, which possibly occur during strong accelerations. Such a situation is often referred to as a μ-jump. Figure 4 shows the time histories of the relative rear wheel slip, vehicle and wheel speeds and driving torque in a traction maneuver on the full multibody simulator where a μ-jump from $\mu = 0.2$ to $\mu = 0.4$ with relative rear slip $\lambda_{r,r}$ as controlled variable. The results in Figure 4 show that the proposed controller can guarantee safety also in very critical maneuvers. Finally, we need to take into account disturbances. As is well known, SM control is very attractive to deal with uncertain systems, but its formulation allows to formally take into account only the so called *matched* disturbances, [15]. However, in the automotive context one has to handle also measurements disturbances, i.e., unmatched ones. Thus, we carried out some simulations in the multibody environment where first only matched disturbances – in the form of a zero-mean white noise on the throttle position – and then also unmatched disturbances – in the form of a zero-mean white noise on the wheel speeds – have been taken into account. The results of these simulations are shown in Figure 5, where the behavior of the relative wheel slip and the driving torque is shown in both cases (the noise intensities used in these simulations is $\sigma^2_{th} = 0.1\%$ and $\sigma^2_{\omega_i} = 0.001 rad^2/s^2$, $i = \{f, r\}$). As can be seen, the closed-loop behavior remains acceptable and safe even in the presence of unmatched disturbances, thereby confirmig the suitability of the proposed SOSM controller for motorcycle traction control applications.

REFERENCES

[1] M. Corno, S. Savaresi, M. Tanelli, and L. Fabbri, "On optimal motorcycle braking." *Control Engineering Practice*, vol. 16, no. 6, pp. 644–657, 2008.

[2] M. Amodeo, A. Ferrara, R. Terzaghi, and C. Vecchio, "Wheel slip control via second order sliding modes generation," in *Conference on Decision and Control, CDC07*, New Orleans, USA, December 12–14 2007.

[3] H. Lee and M. Tomizuka, "Adaptive vehicle traction force control for intelligent vehicle highway systems (ivhss)," *IEEE Transactions on Industrial Electronics*, vol. 50, no. 1, pp. 37–47, 2003.

[4] U. Kiencke and L. Nielsen, *Automotive Control Systems*. Springer-Verlag, Berlin, 2000.

[5] V. Cossalter, *Motorcycle Dynamics*. Milwaukee, USA: Race Dynamics, 2002.

[6] R. S. Sharp, "Stability, control and steering responses of motorcycles," *Vehicle System Dynamics*, vol. 35, pp. 291–318, 2001.

[7] G. Bartolini, A. Ferrara, F. Levant, and E. Usai, "On second order sliding mode controllers," in *Lecture Notes in Control and Information Sciences*, K. D. Young and U. Özgüner, Eds., vol. 247. Berlin: Springer-Verlag, 1999, pp. 329–350.

[8] G. Bartolini, A. Ferrara, and E. Usai, "Chattering avoidance by second-order sliding mode control," *IEEE Transactions on Automatic Control*, vol. 43, no. 2, pp. 241–246, 1998.

[9] M. Tanelli, M. Prandini, F. Codecà, A. Moia, and S. Savaresi, "Analysing the interaction between braking control and speed estimation: the case of two-wheeled vehicles," in *47th IEEE Conference on Decision and Control, Cancun, Mexico*, 2008.

[10] M. Tanelli, A. Astolfi, and S. Savaresi, "Robust nonlinear output feedback control for brake-by-wire control systems." *Automatica*, vol. 44, no. 4, pp. 1078–1087, 2008.

[11] C. Edwards and K. S. Spurgeon, *Sliding mode control: theory and applications*. London, U.K.: Taylor & Francis, 1998.

[12] M. Corno, M. Tanelli, S. Savaresi, L. Fabbri, and L. Nardo, "Electronic throttle control for ride-by-wire in sport motorcycles," in *IEEE Multi-conference on Systems and Control, San Antonio, Texas, USA*, 2008, pp. 233–238.

[13] R. S. Sharp, S. Evangelou, and D. J. N. Limebeer, "Advances in the modelling of motorcycle dynamics," *Multibody System Dynamics*, vol. 12, pp. 251–283, 2004.

[14] I. Boiko, L. Fridman, A. Pisano, and E. Usai, "Performance Analysis of Second-Order Sliding-Mode Control Systems With Fast Actuators," *IEEE Transactions on Automatic Control*, vol. 52, no. 6, pp. 1053–1059, 2007.

[15] V. Utkin, J. Guldner, and J. Shi, *Sliding-Mode Control in Electromechanical Systems*. London, U.K.: Taylor & Francis, 1999.